Ingenieur-Archiv 56 (1986) 254–264

Ingenieur-Archiv

A theory of rotating elasto-plastic shrink fits

U. Gamer, Wien and F. G. Kollmann, Darmstadt

Summary: The paper gives a rigorous theory of rotating elasto-plastic shrink fits under the assumptions of infinitesimal strain, ideal plasticity and validity of Tresca's yield condition. The plastic strain increments are computed by the associated flow rule. Furthermore, it is assumed that the shaft remains purely elastic during the entire loading history. It is shown that, below a limit speed, the plastic deformation is governed by one side of the Tresca hexagon only. Beyond this speed, a second face of Tresca's hexagon becomes involved. In this case plastic prestrains accumulated below the limit speed have to be considered. For both speed regimes, solutions comprising stresses and radial displacement are obtained. Finally a numerical example is given.

Eine Theorie rotierender elastisch-plastischer Preßverbände

Übersicht: Der Aufsatz gibt eine exakte Theorie des rotierenden elasto-plastischen Preßverbandes unter den Voraussetzungen infinitesimaler Verzerrungen, idealer Plastizität und der Gültigkeit der Trescaschen Fließbedingung. Die plastischen Dehnungsinkremente werden nach der zugeordneten Fließregel berechnet. Ferner wird vorausgesetzt, daß die Welle während der vollständigen Belastungsgeschichte rein elastisch bleibt. Es wird gezeigt, daß unterhalb einer Grenzdrehzahl die plastische Deformation von nur einer Seite des Trescaschen Sechsecks bestimmt wird. Oberhalb dieser Drehzahl wird eine zweite Seite des Trescaschen Sechsecks beteiligt. In diesem Fall müssen plastische Vordehnungen berücksichtigt werden, die unterhalb der Grenzdrehzahl entstanden. Für beide Drehzahlbereiche werden Lösungen abgeleitet, welche Spannungen und Radialverschiebung umfassen. Schließlich wird ein numerisches Beispiel angegeben.

1 Introduction

Shrink fits are widely used in mechanical engineering as they offer high transferable loads at favourable production costs. Usually a purely elastic design is applied. The clearance between hub and shaft is chosen in such a way that the stresses in all regions of the fit lie below a limit given by a suitably selected yield criterion. Furthermore, the influence of the centrifugal body force is neglected in the elementary design criteria for shrink fits [1]. They are based on Lamé's solution for the thick-walled elastic pipe assuming a state of plane stress in shaft and hub. The decrease of contact pressure between hub and shaft with angular velocity has been investigated by Biezeno and Grammel [2].

A simple computation reveals that by a purely elastic design the strength of especially the hub material is utilized poorly. This can be improved by an elasto-plastic design. The first solution for a non-rotating elasto-plastic shrink fit was given by Lundberg [3]. He assumed a state of plane stress, infinitesimal strain and an elastic-idealplastic material following v. Mises' yield criterion. Furthermore he applied Hencky's deformation theory. Despite this lack of rigorousness, Lundberg's solution is rather complicated and not very suitable for practical computations.

A solution based on the modern concepts of the theory of plasticity has been derived by Kollmann [4]. He also presupposed plane stress and an elastic-idealplastic material. But he used Tresca's yield criterion and the associated flow rule according to Melan, Prager and Koiter [5].

An extension of Kollmann's theory for workhardening materials has been given by Gamer and Lance [6].

The problem of rotating elasto-plastic shrink fits has been investigated by Kollmann [7]. To avoid complicated case distinctions he confined his work to full shafts remaining purely elastic during the entire deformation history. He further assumed that Young's modulus, Poisson's ratio and the density of the shaft and hub material are equal. He showed that below a limit angular speed ω_l the plastic deformation of the hub material is governed by one of Tresca's yield functions only. For angular velocities beyond ω_l a second side of the Tresca hexagon is involved. Kollmann's solution is correct only for angular velocities up to ω_l. For larger values of the angular velocity he did not consider the plastic predeformation.

It is the aim of the present paper to give a rigorous theory of rotating elasto-plastic shrink fits. A related thermoplastic problem has been solved by Gamer and Mack [8]. Our work is based on the following assumptions: We confine ourselves to full shafts which remain purely elastic during the entire loading history. We presuppose that the elastic moduli E and ν as well as the density ϱ of the shaft and hub material are equal. But the yield stresses σ_{YS} and σ_{YH} of the shaft and hub material can be different. We consider a state of plane stress and assume infinitesimal deformation. As in our prior work we use Tresca's yield criterion and the associated flow rule for the elastic-idealplastic material of the hub.

2 General theory

It is useful to formulate the entire theory in nondimensional form [7]. The state of the system after fitting but before first rotational loading is denoted as the initial state. We consider a shrink fit shown in Fig. 1 with the effective radial clearance Z. It can be shown [7] that, for

$$\Psi := \frac{E}{\sigma_{YH}} \frac{Z}{a} \leqq \frac{3+\nu}{3+\nu+(1-\nu)\,Q^2}, \tag{1}$$

the initial state is purely elastic and the entire hub remains elastic until take-off. With the inner radius a and outer radius b of the hub the parameter Q is defined as

$$Q := \frac{a}{b}. \tag{2}$$

Next we define a nondimensional angular speed

$$\Omega := a\omega \sqrt{\frac{\varrho}{\sigma_{YH}}}. \tag{3}$$

The purely elastic take-off speed is given by

$$\Omega_T = 2Q \sqrt{\frac{\Psi}{3+\nu}}. \tag{4}$$

Where no ambiguity can arise we will omit the index H for the hub material in the sequel. For

$$\frac{3+\nu}{3+\nu+(1-\nu)\,Q^2} < \Psi < 1 \tag{5}$$

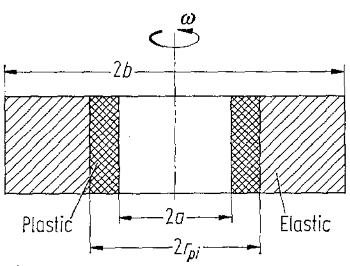

Fig. 1. Cross section of rotating elasto-plastic shrink fit

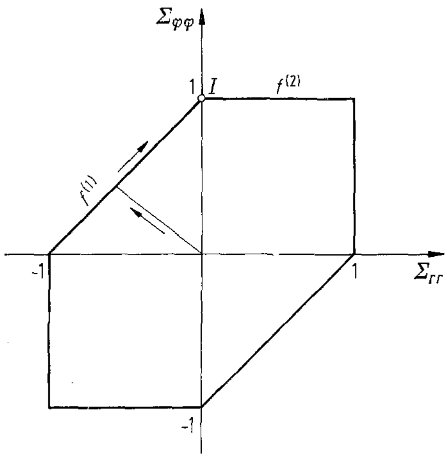

Fig. 2. Tresca's yield condition for plane stress

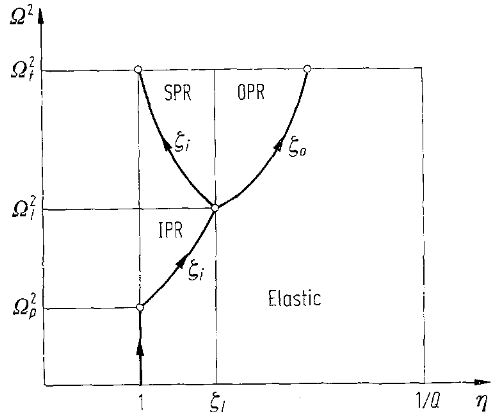

Fig. 3. Schematic sketch of dependence of plasticity radii ζ_i and ζ_o on Ω^2

the initial state is still purely elastic but plastic deformation can occur during rotational loading. In this case first plastic flow sets on at the bore of the hub ($r = a$) for

$$\Omega_p = 2\sqrt{\frac{1-\Psi}{1-\nu}}. \tag{6}$$

It has to be observed that Ω_p is independent of the radii ratio Q. For $\Psi > 1$ the initial state is elasto-plastic.

Next we define nondimensional stresses in the hub

$$\Sigma_{rr} := \frac{\sigma_{rr}}{\sigma_{YH}}, \qquad \Sigma_{\varphi\varphi} := \frac{\sigma_{\varphi\varphi}}{\sigma_{YH}}, \tag{7}$$

where σ_{rr} and $\sigma_{\varphi\varphi}$ are the radial and circumferential stresses. It can be shown [7] that, for a purely elastic as well as an elasto-plastic initial state for limited values of Ω, the plastic deformation of the hub is governed by Tresca's yield function $f^{(1)}$ only (Fig. 2):

$$f^{(1)} = -\Sigma_{rr} + \Sigma_{\varphi\varphi} - 1. \tag{8}$$

The meaning of limited Ω will be made precise later.

Let us assume that condition (5) holds and that the angular speed is increased monotonically. Then Ω^2 can be considered as a loading parameter. In Fig. 3 the development of plastic zones in the hub with Ω^2 is shown. The quantity $\eta := r/a$ is a nondimensional radius. The hub covers the interval $1 \leqq \eta \leqq 1/Q$. Up to Ω_p the entire hub remains purely elastic. For $\Omega = \Omega_p$ the hub becomes plastic at the bore. For increased velocity a plastic zone spreads outward radially and extends between $1 \leqq \eta \leqq \zeta_i$, where $\zeta_i := r_{pi}/a$ is the nondimensional plasticity radius. We denote this plastic zone as inner plastic region (IPR) for reasons which will become obvious later.

The stresses in the IPR are governed by the Eq. of equilibrium

$$\frac{d\Sigma_{rr}}{d\eta} + \frac{\Sigma_{rr} - \Sigma_{\varphi\varphi}}{\eta} = -\Omega^2\eta \tag{9}$$

and Tresca's yield condition $f^{(1)} = 0$ (compare (8)). The general solution is

$$\Sigma_{rr} = \ln\eta - \frac{\Omega^2}{2}\eta^2 + C_1, \qquad \Sigma_{\varphi\varphi} = 1 + \ln\eta - \frac{\Omega^2}{2}\eta^2 + C_1, \tag{10}$$

where C_1 is an "integration constant" which depends on the loading parameter Ω^2.

The associated flow rule [9] leads to the plastic strain increments

$$\mathrm{d}\varepsilon_{rr}^p = -\mathrm{d}\lambda_1, \qquad \mathrm{d}\varepsilon_{\varphi\varphi}^p = \mathrm{d}\lambda_1, \qquad \mathrm{d}\varepsilon_{zz}^p = 0. \tag{11}$$

Here $\mathrm{d}\lambda_1$ is a nonnegative parameter. From (11) there follows

$$\mathrm{d}\varepsilon_{rr}^p + \mathrm{d}\varepsilon_{\varphi\varphi}^p = 0. \tag{12}$$

Therefore the sum of the total radial and circumferential strain increments is purely elastic:

$$\mathrm{d}\varepsilon_{rr} + \mathrm{d}\varepsilon_{\varphi\varphi} = \frac{(1-\nu)\,\sigma_Y}{E}\,(\mathrm{d}\Sigma_{rr} + \mathrm{d}\Sigma_{\varphi\varphi}). \tag{13}$$

Eq. (13) leads in a natural way to the definition of scaled strains

$$\bar{\varepsilon}_{rr} := \frac{E}{\sigma_Y}\,\varepsilon_{rr}, \qquad \bar{\varepsilon}_{\varphi\varphi} := \frac{E}{\sigma_Y}\,\varepsilon_{\varphi\varphi}. \tag{14}$$

Integration of (13) with respect to the loading parameter Ω^2 under consideration of (10) gives

$$\bar{\varepsilon}_{rr} + \bar{\varepsilon}_{\varphi\varphi} = (1-\nu)\,(1 + 2\ln\eta - \Omega^2\eta^2 + 2C_1) + F(\eta). \tag{15}$$

Here, $F(\eta)$ is an undetermined function depending on the nondimensional radius η but not on the loading parameter Ω^2. Physically it represents the sum of plastic prestrains in radial and circumferential direction. But since the hub has not undergone any plastic prestraining, these plastic prestrains vanish in the entire IPR and therefore $F(\eta) = 0$.

Next we define a nondimensional radial displacement

$$\bar{u} := \frac{E}{\sigma_Y}\,\frac{u}{a}, \tag{16}$$

where u is the radial displacement. Then the strain-displacement-relations and (15) lead to a differential Eq. for $\bar{u}$ with the general solution

$$\bar{u} = (1-\nu)\left(\eta\ln\eta - \frac{\Omega^2}{4}\,\eta^3 + C_1\eta\right) + \frac{C_2}{\eta}. \tag{17}$$

Here C_2 again is an "integration constant" depending on Ω^2.

The stresses and the displacement in the elastic region $\zeta_1 \leqq \eta \leqq 1/Q$ are given by

$$\begin{aligned}
\Sigma_{rr} &= -\frac{K_1}{\eta^2} + K_2 - \frac{3+\nu}{8}\,(\Omega\eta)^2, \\
\Sigma_{\varphi\varphi} &= \frac{K_1}{\eta^2} + K_2 - \frac{1+3\nu}{8}\,(\Omega\eta)^2, \\
\bar{u} &= (1+\nu)\,\frac{K_1}{\eta} + (1-\nu)\,K_2\eta - \frac{1-\nu^2}{8}\,\Omega^2\eta^3,
\end{aligned} \tag{18}$$

where K_1 and K_2 are "integration constants" depending on Ω^2. The solution for the purely elastic shaft can be derived from (18) by setting $K_1 = 0$ and substituting K_2 by K_3

The unknowns C_1, C_2, K_1, K_2, K_3 and the plasticity radius ζ_i have to be computed from the following boundary and transition conditions, where the superscript E denotes the elastic, I the inner plastic region and S the shaft:

$$\bar{u}^I(1) - \bar{u}^S(1) = \Psi, \tag{19}$$

$$\Sigma_{rr}^S(1) = \Sigma_{rr}^I(1), \tag{20}$$

$$\Sigma_{rr}^I(\zeta_i) = \Sigma_{rr}^E(\zeta_i), \tag{21}$$

$$\Sigma_{\varphi\varphi}^I(\zeta_i) = \Sigma_{\varphi\varphi}^E(\zeta_i), \tag{22}$$

$$\bar{u}^I(\zeta_i) = \bar{u}^E(\zeta_i), \tag{23}$$

$$\Sigma_{rr}^E(1/Q) = 0. \tag{24}$$

The radial displacement of the surface of the shaft is given by [7]

$$\bar{u}^S(1) = (1-\nu)\left[-\ln\zeta_i + \frac{\Omega^2}{2}\left(\zeta_i^2 - \frac{1}{2}\right)\right]. \tag{25}$$

After some algebra the following expressions for the stresses and the displacement in the hub are found.

Inner plastic region $(1 \leqq \eta \leqq \zeta_i)$

$$\Sigma_{rr} = -\frac{1}{2}\left[1 + 2\ln\frac{\zeta_i}{\eta} - (Q\zeta_i)^2\right] - \frac{1}{2}(\Omega\eta)^2 + \frac{1-\nu}{4}(\Omega\zeta_i)^2 + \frac{1}{8}\left(\frac{\Omega}{Q}\right)^2 [3 + \nu - (1-\nu)(Q\zeta_i)^4], \tag{26}$$

$$\Sigma_{\varphi\varphi} = -\frac{1}{2}\left[-1 + 2\ln\frac{\zeta_i}{\eta} - (Q\zeta_i)^2\right] - \frac{1}{2}(\Omega\eta)^2 + \frac{1-\nu}{4}(\Omega\zeta_i)^2 + \frac{1}{8}\left(\frac{\Omega}{Q}\right)^2 [3 + \nu - (1-\nu)(Q\zeta_i)^4], \tag{27}$$

$$\bar{u} = (1-\nu)\,\eta\left\{-\frac{1}{2}\left[1 + 2\ln\frac{\zeta_i}{\eta} - (Q\zeta_i)^2\right] + \frac{1-\nu}{8}(\Omega\zeta_i)^2[2 - (Q\zeta_i)^2] + \frac{3+\nu}{8}\left(\frac{\Omega}{Q}\right)^2 - \frac{1}{4}(\Omega\eta)^2\right\} + \frac{\Psi}{\eta}. \tag{28}$$

Elastic region $(\zeta_i \leqq \eta \leqq 1/Q)$

$$\Sigma_{rr} = \frac{\zeta_i^2}{2\eta^2}[1 - (Q\eta)^2]\left[-1 + \frac{1-\nu}{4}(\Omega\zeta_i)^2\right] + \frac{3+\nu}{8}\left(\frac{\Omega}{Q}\right)^2 [1 - (Q\eta)^2], \tag{29}$$

$$\Sigma_{\varphi\varphi} = -\frac{\zeta_i^2}{2\eta^2}[1 + (Q\eta)^2]\left[-1 + \frac{1-\nu}{4}(\Omega\zeta_i)^2\right] + \frac{3+\nu}{8}\left(\frac{\Omega}{Q}\right)^2\left[1 - \frac{1+3\nu}{3+\nu}(Q\eta)^2\right], \tag{30}$$

$$\bar{u} = \frac{\eta}{2}\left\{\left[1 - \frac{1-\nu}{4}(\Omega\zeta_i)^2\right]\left[(1+\nu)\left(\frac{\zeta_i}{\eta}\right)^2 + (1-\nu)(Q\zeta_i)^2\right] + \frac{3+\nu}{4}\left(\frac{\Omega}{Q}\right)^2\left[1 - \nu - \frac{1-\nu^2}{3+\nu}(Q\eta)^2\right]\right\}. \tag{31}$$

The stresses and displacement in the shaft are omitted here for the sake of brevity.

The nondimensional plasticity radius ζ_i is determined from (19). This leads to the following equation

$$\Psi - \zeta_i^2 + \frac{1-\nu}{4}\Omega^2\zeta_i^4 = 0 \tag{32}$$

with the root

$$\zeta_i = \frac{1}{\Omega}\sqrt{\frac{2}{1-\nu}\left(1 - \sqrt{1 - (1-\nu)\,\Omega^2\Psi}\right)}. \tag{33}$$

It is remarkable that the plasticity radius depends only on the parameter Ψ and on the nondimensional angular speed Ω but not on the radii ratio Q. For a given hub material and a given clearance Z, ζ_i is a function of Ω only for all possible geometrical configurations of hub and shaft.

The solution (26) to (33) is valid as long as all material points of the hub have images on Tresca's yield surface $f^{(1)} = 0$ in stress space. If $\Sigma_{rr} > 0$ the image can not lie on $f^{(1)} = 0$ anymore. Therefore from $\Sigma_{rr}^I(\zeta_l, \Omega_l) = 0$ a limit condition for the validity of the solution derived can be obtained. Here ζ_l denotes the nondimensional limit plasticity radius which is reached at the limit speed Ω_l (Fig. 3). For $\Omega = \Omega_l$ the image of the material point $\eta = \zeta_l$ lies in stress space in the corner I of Tresca's hexagon. A straightforward computation leads to the equations

$$\Omega_l = 2Q \sqrt{\frac{1}{3+\nu}\left(1 - \frac{1-\nu}{3+\nu} Q^2\Psi\right)}, \tag{34}$$

$$\zeta_l = \sqrt{\frac{\Psi}{1 - \frac{1-\nu}{3+\nu} Q^2\Psi}}. \tag{35}$$

Next let us consider the case $\Omega > \Omega_l$. Then we have to distinguish three plastic zones. In the inner plastic region (IPR) $1 \leqq \zeta_i$ the yield function $f^{(1)}$ governs the plastic deformation. For $\zeta_i \leqq \eta \leqq \zeta_o$ the yield function $f^{(2)}$ has to be considered. But careful attention has to be paid to the plastic deformation. In the region $\zeta_i \leqq \eta \leqq \zeta_l$, which we denote as special plastic region (SPR), prior plastic deformations governed by $f^{(1)}$ have to be taken into account. The material points in the SPR have undergone plastic deformations for speeds $\Omega_p < \Omega \leqq \Omega_l$. Only the increase of the plastic deformation beyond the predeformation is governed by Tresca's yield function $f^{(2)}$. Finally in the outer plastic region (OPR) $\zeta_l \leqq \eta \leqq \zeta_o$, material is becoming plastic which for $\Omega \leqq \Omega_l$ no previous plastic deformation has seen. The outer plasticity radius ζ_o marks the boundary between the plastic and elastic region.

For the IPR the stresses (10) and the displacement (17) can be maintained if new "integration constants", $C_1 \to C_3$ and $C_2 \to C_4$, are introduced. Next let us inspect the SPR and determine the stresses in it. They can be computed from the equilibrium condition (9) and the yield condition

$$f^{(2)} = \Sigma_{\varphi\varphi} - 1 = 0. \tag{36}$$

The solution further has to meet the condition

$$\Sigma_{rr}(\zeta_i) = 0. \tag{37}$$

The adjusted solution is

$$\Sigma_{rr} = 1 - \frac{\zeta_i}{\eta} + \frac{1}{3}(\Omega\zeta_i)^2 \left[\frac{\zeta_i}{\eta} - \left(\frac{\eta}{\zeta_i}\right)^2\right], \qquad \Sigma_{\varphi\varphi} = 1. \tag{38}$$

The boundary between the IPR and the SPR is $\eta = \zeta_i$ where ζ_i is a function $\zeta_i(\Omega)$ of the angular speed Ω. Due to (37) the image of the material point $\eta = \zeta_i$ lies in stress space at the corner I (Fig. 2). Let us denote by $\Omega_c(\eta)$ the angular velocity at which the image of a material point situated at the radius η reaches the corner I in stress space. The function $\Omega_c(\eta)$ is the inverse of the function $\zeta_i(\Omega)$. As for $\Omega = \Omega_c(\eta)$ the image of the material point at η reaches the corner I in stress space, the following conditions for the stresses hold

$$\Sigma_{rr}[\eta, \Omega_c(\eta)] = 0, \qquad \Sigma_{\varphi\varphi}[\eta, \Omega_c(\eta)] = 1. \tag{39}$$

After these preliminaries we now can investigate the deformation in the SPR. For $\Omega = \Omega_c(\eta)$ the total radial strain which a material point at the radius η has undergone can be expressed as

$$\bar{\varepsilon}_{rr}[\eta, \Omega_c(\eta)] = \bar{\varepsilon}_{rr}^E[\eta, \Omega_c(\eta)] + \bar{\varepsilon}_{rr}^{\text{per}}(\eta). \tag{40}$$

The superscript E indicates elastic deformation. The quantity $\bar{\varepsilon}_{rr}^{\text{per}}(\eta)$ is the permanent plastic strain which has developed for angular speed $\Omega_p(\eta) < \Omega \leqq \Omega_c(\eta)$ and has been governed by the yield function $f^{(1)}$. At the angular velocity $\Omega_p(\eta)$ plastic deformation sets on at the radius η. Therefore $\bar{\varepsilon}_{rr}^{\text{per}}(\eta)$ is the radial plastic strain of the material point at η accumulated until its image reaches the corner I in stress space. If the angular velocity is increased $(\Omega > \Omega_c(\eta))$ the permanent plastic strain $\bar{\varepsilon}_{rr}^{\text{per}}(\eta)$ at the radius η is not increased, since all further plastic deformation is governed by the yield function $f^{(2)}$. The plastic strain increments for $\Omega > \Omega_c(\eta)$ are obtained by the associated flow rule and the yield function $f^{(2)}$ as

$$\mathrm{d}\bar{\varepsilon}_{rr}^p = 0, \qquad \mathrm{d}\bar{\varepsilon}_{\varphi\varphi}^p = \mathrm{d}\lambda_2, \qquad \mathrm{d}\bar{\varepsilon}_{zz}^p = -\mathrm{d}\lambda_2, \tag{41}$$

where again $\mathrm{d}\lambda_2$ is a nonnegative parameter. Since the radial plastic strain increment vanishes, the total radial strain increment is purely elastic. Therefore the increase of the radial strain in the interval $(\Omega_c, \Omega]$ is obtained as

$$\bar{\varepsilon}_{rr}(\eta, \Omega) - \bar{\varepsilon}_{rr}[\eta, \Omega_c(\eta)] = \Sigma_{rr}(\eta, \Omega) - \nu[\Sigma_{\varphi\varphi}(\eta, \Omega) - 1], \tag{42}$$

where Eqs. (39) have been observed. From (39) there follows

$$\bar{\varepsilon}_{rr}^{E}[\eta, \Omega_c(\eta)] = -\nu. \tag{43}$$

Equations (42), (40) and (43) lead to

$$\bar{\varepsilon}_{rr}(\eta, \Omega) = \Sigma_{rr}(\eta, \Omega) - \nu\Sigma_{\varphi\varphi}(\eta, \Omega) + \bar{\varepsilon}_{rr}^{\mathrm{per}}(\eta). \tag{44}$$

Considering the strain-displacement-relation, (44) can be interpreted as a differential equation for the radial displacement $\bar{u}$ which can be easily integrated after insertion of the stresses (38),

$$\bar{u} = \eta\left\{1 - \nu + \left[\frac{1}{3}(\Omega\zeta_i)^2 - 1\right]\frac{\zeta_i}{\eta}\ln\eta\right\} + \int_{\zeta_i}^{\eta} \bar{\varepsilon}_{rr}^{\mathrm{per}}(\chi)\, d\chi + C_5 \tag{45}$$

with a new "integration constant" C_5.

From (45) the total circumferential strain is obtained as

$$\bar{\varepsilon}_{\varphi\varphi} = 1 - \nu + \left[\frac{1}{3}(\Omega\zeta_i)^2 - 1\right]\frac{\zeta_i}{\eta}\ln\eta + \frac{1}{\eta}\left(\int_{\zeta_i}^{\eta} \bar{\varepsilon}_{rr}^{\mathrm{per}}(\chi)\, d\chi + C_5\right). \tag{46}$$

The elastic circumferential strain follows from the stresses (38) and, after a straightforward computation, the plastic circumferential strain

$$\begin{aligned}\bar{\varepsilon}_{\varphi\varphi}^{p}(\eta, \Omega) = &-\frac{1 + 3\nu}{9}(\Omega\eta)^2 + \left[\frac{1}{3}(\Omega\zeta_i)^2 - 1\right]\frac{\zeta_i}{\eta}(\ln\eta + \nu) \\ &+ \frac{1}{\eta}\left(\int_{\zeta_i}^{\eta} \bar{\varepsilon}_{rr}^{\mathrm{per}}(\chi)\, d\chi + C_5\right)\end{aligned} \tag{47}$$

is obtained.

At the boundary $\eta = \zeta_i$ between the IPR and the SPR the plastic strains also have to meet the integrated form of (11). Therefore

$$\bar{\varepsilon}_{\varphi\varphi}^{p}(\zeta_i, \Omega) = -\bar{\varepsilon}_{rr}^{p}(\zeta_i, \Omega) \tag{48}$$

must hold. In (48) it has to be observed that ζ_i depends on Ω. Next we conclude that

$$\bar{\varepsilon}_{rr}^{p}(\zeta_i, \Omega) = \bar{\varepsilon}_{rr}^{\mathrm{per}}(\zeta_i), \tag{49}$$

since at the interface between the IPR and the SPR the radial plastic strain is just equal to the permanent radial plastic strain accumulated in the interval $[\Omega_p(\eta), \Omega_c(\eta)]$ by plastic deformation governed by the yield function $f^{(1)}$. From (47–49) the "integration constant" C_5 can be determined. After some algebra, the radial displacement in the SPR is obtained as

$$\begin{aligned}\bar{u} = &(1 - \nu)\,\eta + \nu\zeta_i - \zeta_i\ln\frac{\eta}{\zeta_i} - \frac{\Omega^2}{9}(\eta^3 - \zeta_i^3) \\ &- \frac{\Omega^2}{3}\zeta_i^3\ln\frac{\zeta_i}{\eta} - \zeta_i\bar{\varepsilon}_{rr}^{\mathrm{per}}(\zeta_i) + \int_{\zeta_i}^{\eta} \bar{\varepsilon}_{rr}^{\mathrm{per}}(\chi)\, d\chi.\end{aligned} \tag{50}$$

We recall that in the SPR the stresses are given by (38). Therefore the stresses and the radial displacement are determined as function of the radius η, the angular speed Ω and by the still unknown functions $\zeta_i(\Omega)$ and $\bar{\varepsilon}_{rr}^{\mathrm{per}}(\eta)$.

Next the "integration constants" C_3 and C_4 for the IPR can be determined. The "integration constant" C_3 follows from (37) and C_4 from the continuity of the radial displacement at the interface $\eta = \zeta_i$ between IPR and SPR. We suppress the stresses and displacement here and rather collect the complete solution for $\Omega \geqq \Omega_l$ later (59—67).

In the OPR the stresses (38) are valid since for both the SPR and OPR the yield function $f^{(2)}$ is relevant. For the radial displacement the solution (45) can be adopted with $\bar{\varepsilon}_{rr}^{\text{per}} = 0$, since in the OPR no plastic predeformation governed by $f^{(1)}$ is present. Of course, the "integration constant" C_5 has to be substituted by a new one C_6. This can be determined from the condition of continuity for the radial displacement at the interface $\eta = \zeta_l$ between SPR and OPR.

In the elastic region $\zeta_o \leqq \eta \leqq 1/Q$ the solution (18) is valid with new "integration constants", $K_1 \to K_5$ and $K_2 \to K_6$. The solution for the shaft is obtained from (18) by setting $K_1 = 0$ and substituting K_2 by K_4.

The not yet determined unknowns are the "integration constants" K_4, K_5, K_6 and the functions $\zeta_i(\Omega)$, $\zeta_o(\Omega)$, $\bar{\varepsilon}_{rr}^{\text{per}}(\eta)$. They can be determined from (19, 20) and the following continuity and boundary conditions:

$$\Sigma_{rr}^O(\zeta_o) = \Sigma_{rr}^E(\zeta_o), \quad (51) \qquad \Sigma_{\varphi\varphi}^O(\zeta_o) = \Sigma_{\varphi\varphi}^E(\zeta_o), \quad (52)$$

$$\bar{u}^O(\zeta_o) = \bar{u}^E(\zeta_o), \quad (53) \qquad \Sigma_{rr}^E(1/Q) = 0. \quad (54)$$

Here the superscript O denotes the OPR. For the lengthy computations we used MACSYMA [10], a computer algebra system. It led to the following equations:

$$\left[\frac{1}{3}(\Omega\zeta_i)^2 - 1\right]\frac{\zeta_i}{\zeta_o}\ln\frac{\zeta_o}{\zeta_i} - \frac{1+3\nu}{9}(\Omega\zeta_o)^2\left[1 - \left(\frac{\zeta_i}{\zeta_o}\right)^3\right]$$
$$- \frac{\zeta_i}{\zeta_o}\bar{\varepsilon}_{rr}^{\text{per}}(\zeta_i) + \frac{1}{\zeta_o}\int_{\zeta_i}^{\zeta_l}\bar{\varepsilon}_{rr}^{\text{per}}(\chi)\,d\chi = 0, \quad (55)$$

$$\left[1 - \frac{1-\nu}{4}(\Omega\zeta_i)^2 - \bar{\varepsilon}_{rr}^{\text{per}}(\zeta_i)\right]\zeta_i^2 = \Psi, \quad (56)$$

$$\frac{2}{1+(Q\zeta_o)^2} - \frac{\zeta_i}{\zeta_o} + \frac{1+3\nu}{12}\,\frac{2-(Q\zeta_o)^2}{1+(Q\zeta_o)^2}(\Omega\zeta_o)^2$$
$$+ \frac{1}{3}\frac{\zeta_i}{\zeta_o}(\Omega\zeta_i)^2 - \frac{3+\nu}{4}\,\frac{1}{1+(Q\zeta_o)^2}\left(\frac{\Omega}{Q}\right)^2 = 0. \quad (57)$$

Equations (55—57) have to be solved numerically for the unknowns ζ_i, ζ_o and $\bar{\varepsilon}_{rr}^{\text{per}}(\zeta_i)$ depending on the load parameter Ω which is the independent variable of the problem. But this direct approach proved insufficient in so far as, due to numerical inaccuracies, small discontinuities of the displacement and the plastic strains at the boundary $\eta = \zeta_o$ between the plastic and elastic region occurred. Therefore the following approach was used.

We consider ζ_i as independent variable and solve the system for Ω^2, $\bar{\varepsilon}_{rr}^{\text{per}}(\zeta_i)$ and ζ_o. First Ω^2 is computed from (57) and inserted into (55) and (56). Then (55), which is a Volterra integral equation of the second kind for the unknown $\bar{\varepsilon}_{rr}^{\text{per}}(\zeta_i)$, is differentiated with respect to ζ_i and thus reduced to an ordinary differential equation of order one. It contains the unknowns ζ_o and $\bar{\varepsilon}_{rr}^{\text{per}}(\zeta_i)$ and their first derivatives with respect to ζ_i. Then, using (56), $\bar{\varepsilon}_{rr}^{\text{per}}(\zeta_i)$ and its derivative are eliminated. The result is a differential equation for ζ_o of the form

$$\frac{d\zeta_o}{d\zeta_i} - f(\zeta_i, \zeta_o) = 0. \quad (58)$$

Here $f(\zeta_i, \zeta_o)$ is a very lengthy nonlinear function of ζ_i and ζ_o. For its generation again MACSYMA has been used. The expression for $f(\zeta_i, \zeta_o)$ has been transformed directly into FORTRAN by MACSYMA. Equation (58) then has been solved numerically by a standard Runge-Kutta routine with $\zeta_o = \zeta_l$ as initial value for $\zeta_i = \zeta_l$. From this numerical solution, sets $\{\zeta_i, \zeta_o, \Omega, \bar{\varepsilon}_{rr}^{\text{per}}(\zeta_i)\}$ in the solution space have been obtained. Once this solution is known the stresses and the radial displacement in the hub can be determined from the following equations.:

Inner plastic region $(1 \leqq \eta \leqq \zeta_i)$

$$\Sigma_{rr} = -\ln \frac{\zeta_i}{\eta} + \frac{\Omega^2}{2} (\zeta_i^2 - \eta^2), \tag{59}$$

$$\Sigma_{\varphi\varphi} = 1 - \ln \frac{\zeta_i}{\eta} + \frac{\Omega^2}{2} (\zeta_i^2 - \eta^2), \tag{60}$$

$$\bar{u} = (1 - \nu) \left[-\ln \frac{\zeta_i}{\eta} + \frac{\Omega^2}{2} \left(\zeta_i^2 - \frac{\eta^2}{2}\right)\right] \eta + \left[1 - \frac{1 - \nu}{4} (\Omega\zeta_i)^2 - \bar{\varepsilon}_{rr}^{\text{per}}(\zeta_i)\right] \frac{\zeta_i^2}{\eta}. \tag{61}$$

Special plastic region $(\zeta_i \leqq \eta \leqq \zeta_l)$

$$\Sigma_{rr} = 1 - \frac{\zeta_i}{\eta} - \frac{(\Omega\eta)^2}{3} \left[1 - \left(\frac{\zeta_i}{\eta}\right)^3\right], \tag{62}$$

$$\Sigma_{\varphi\varphi} = 1, \tag{63}$$

$$\bar{u} = (1 - \nu) \eta + \nu\zeta_i - \frac{\Omega^2}{9} (\eta^3 - \zeta_i^3) - \left[1 - \frac{(\Omega\zeta_i)^2}{3}\right] \zeta_i \ln \frac{\eta}{\zeta_i} - \zeta_i \bar{\varepsilon}_{rr}^{\text{per}}(\zeta_i) + \int_{\zeta_i}^{\eta} \bar{\varepsilon}_{rr}^{\text{per}}(\chi)\, d\chi. \tag{64}$$

Outer plastic region $(\zeta_l \leqq \eta \leqq \zeta_o)$

For the stresses Eqs. (62) and (63) are maintained. For computation of $\bar{u}$ replace in (64) in the integral over $\bar{\varepsilon}_{rr}^{\text{per}}$ the upper boundary η by ζ_l.

Elastic region $(\zeta_o \leqq \eta \leqq 1/Q)$

$$\Sigma_{rr} = -\frac{(\zeta_o/\eta)^2}{1 + (Q\zeta_o)^2} \left[1 - \frac{3 + \nu}{8} \left(\frac{\Omega}{Q}\right)^2 + \frac{1 + 3\nu}{8} (\Omega\zeta_o)^2\right] + \frac{3 + \nu}{8} \frac{(\Omega/Q)^2}{1 + (Q\zeta_o)^2} + \frac{(Q\zeta_o)^2}{1 + (Q\zeta_o)^2} \left[1 + \frac{1 + 3\nu}{8} (\Omega\zeta_o)^2\right] - \frac{3 + \nu}{8} (\Omega\eta)^2, \tag{65}$$

$$\Sigma_{\varphi\varphi} = \frac{(\zeta_o/\eta)^2}{1 + (Q\zeta_o)^2} \left[1 - \frac{3 + \nu}{8} \left(\frac{\Omega}{Q}\right)^2 + \frac{1 + 3\nu}{8} (\Omega\zeta_o)^2\right] + \frac{3 + \nu}{8} \frac{(\Omega/Q)^2}{1 + (Q\zeta_o)^2} + \frac{(Q\zeta_o)^2}{1 + (Q\zeta_o)^2} \left[1 + \frac{1 + 3\nu}{8} (\Omega\zeta_o)^2\right] - \frac{1 + 3\nu}{8} (\Omega\eta)^2, \tag{66}$$

$$\bar{u} = \frac{\eta}{1 + (Q\zeta_o)^2} \left\{(1 + \nu) \left(\frac{\zeta_o}{\eta}\right)^2 \left[1 - \frac{3 + \nu}{8} \left(\frac{\Omega}{Q}\right)^2 + \frac{1 + 3\nu}{8} (\Omega\zeta_o)^2\right] + (1 - \nu) (Q\zeta_o)^2 \left[1 + \frac{3 + \nu}{8(Q\zeta_o)^2} \left(\frac{\Omega}{Q}\right)^2 + \frac{1 + 3\nu}{8} (\Omega\zeta_o)^2\right] - \frac{1 - \nu^2}{8} (\Omega\eta)^2 [1 + (Q\zeta_o)^2]\right\}. \tag{67}$$

3 Numerical results

As a test example we consider a shrink fit with $Q = 0.3$ and $\Psi = 1.2$. According to (5) the initial state of the hub is elasto-plastic. Figure 4 shows the dependence of the pressure P on the angular speed Ω. It resembles the wellknown parabolic distribution for the purely elastic case. Figure 5 presents the development of the plasticity radii ζ_i and ζ_o with Ω. Up to $\Omega = \Omega_l = 0.3265$ only the IPR has developed with the plasticity radius ζ_i which for this case marks the boundary between the IPR and the elastic region. For $\Omega \leqq \Omega_l$ only a relatively weak dependence of ζ_i on Ω can be observed. For $\Omega > \Omega_l$ the SPR and OPR develop. The IPR decreases and so does ζ_i. The plasticity radius ζ_o indicating the boundary between the OPR and the elastic region increases rapidly with Ω.

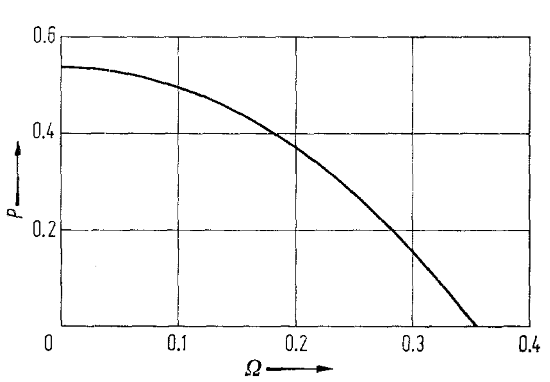

Fig. 4. Dependence of pressure P on angular velocity Ω ($Q = 0.3$; $\Psi = 1.2$)

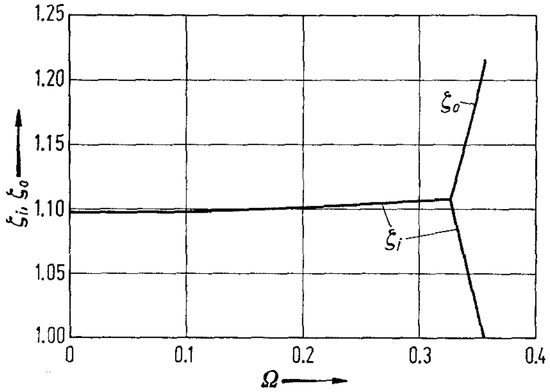

Fig. 5. Dependence of plasticity radii ζ_i and ζ_o on angular velocity Ω ($Q = 0.3$; $\Psi = 1.2$)

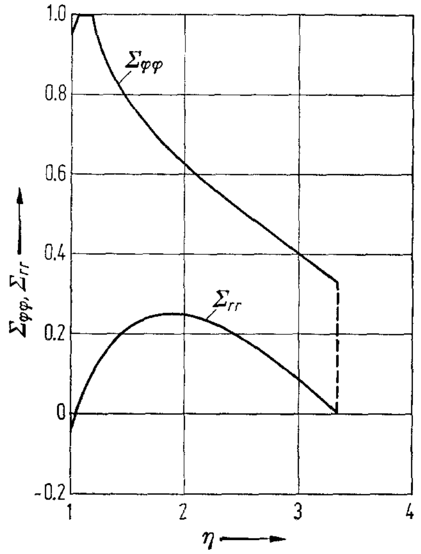

Fig. 6. Distribution of stresses Σ_{rr} and $\Sigma_{\varphi\varphi}$ over radius η ($Q = 0.3$; $\Psi = 1.2$; $\Omega = 0.3400$)

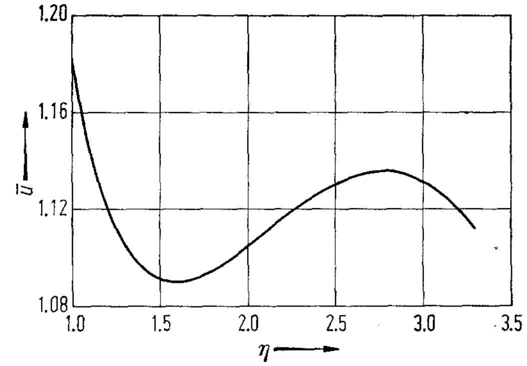

Fig. 7. Distribution of radial displacement $\bar{u}$ over radius η ($Q = 0.3$; $\Psi = 1.2$; $\Omega = 0.3400$)

Figure 6 gives the distribution of the stresses Σ_{rr} and $\Sigma_{\varphi\varphi}$ over the radius η for $\Omega = 0.3400$. The domain, where $\Sigma_{\varphi\varphi} = 1$, covers the SPR and OPR and the stresses meet the yield condition $f^{(2)} = 0$. Figure 7 shows the dependence of the radial displacement $\bar{u}$ on η for $\Omega = 0.3400$. Finally, in Fig. 8 the plastic strains are shown. The Eqs. for the plastic strains can be easily computed and are omitted here for the sake of brevity. In the IPR no axial plastic strain has developed, since the plastic deformation is governed by the yield function $f^{(1)}$. In the SPR plastic strains in all three principal directions can be observed. The radial plastic strain is $\bar{\varepsilon}_{rr}^{\text{per}}$ which has developed for $\Omega \leqq \Omega_c(\eta)$ under the yield function $f^{(1)}$. Since the plastic deformation for a material element at radius η is governed by $f^{(2)}$ for $\Omega > \Omega_c(\eta)$, axial and circumferential strains develop. At the boundary ζ_t between SPR and OPR the radial plastic strain vanishes. The plastic strains in the OPR have developed only under the yield function $f^{(2)}$.

Acknowledgements

The main part of this research has been performed while the authors have been visitors of the Department of Theoretical and Applied Mechanics of Cornell University, Ithaca, N.Y., USA. We gratefully acknowledge the hospitality of this department. Special thanks are due to Professor R. H. Rand for his advice in the application of MACSYMA. The numerical computations have been performed by the Computer Center of Technische Hochschule Darmstadt. Dipl.-Ing. C. Preussner performed the lengthy MACSYMA computations eading to Eq. (58). Mrs. B. Jochem has written the FORTRAN code.

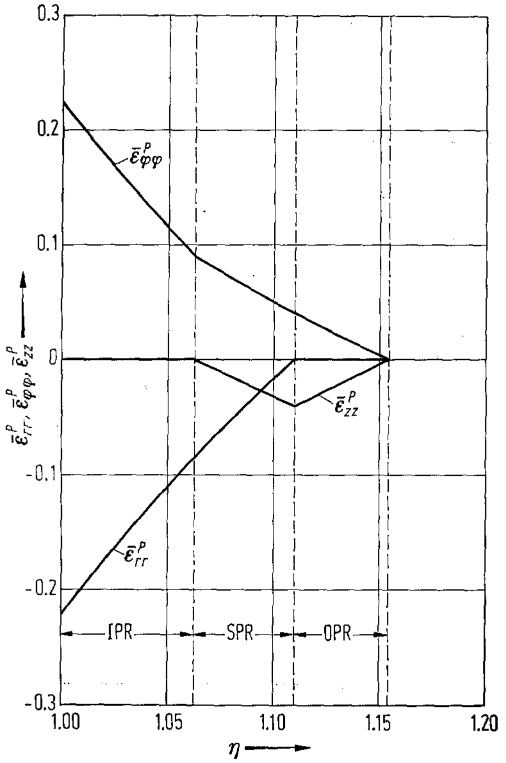

Fig. 8. Distribution of plastic strains over radius η ($Q = 0.3$; $\Psi = 1.2$; $\Omega = 0.3400$)

References

1. Kollmann, F. G.: Welle-Nabe-Verbindungen. Berlin, Heidelberg, New York, Tokyo: Springer 1984
2. Biezeno, C. B.; Grammel, R.: Technische Dynamik, 2nd ed., Vol. 2. Berlin, Heidelberg, New York: Springer 1971
3. Lundberg, G.: Die Festigkeit von Preßsitzen. Das Kugellager 19 (1944) 1—11
4. Kollmann, F. G.: Die Auslegung elastisch-plastisch beanspruchter Querpreßverbände. Forsch. Ing.-Wes. 44 (1978) 1—11
5. Koiter, T. W.: General theorems for elastic-plastic solids. In: Progress in solid mechanics Vol. 1, Amsterdam: North Holland 1960
6. Gamer, U.; Lance, R.: Elastisch-plastische Spannungen im Schrumpfsitz. Forsch. Ing.-Wes. 48 (1982) 192—198
7. Kollmann, F. G.: Rotating elasto-plastic interference fits. Trans. ASME, J. Mech. Des. 103 (1981) 61—66
8. Gamer, U.; Mack, W.: Thermal stress in an elastic-plastic disk exposed to a circular heat source. ZAMP 36 (1985) 568—580
9. Ismar, H.; Mahrenholz, O.: Technische Plastomechanik. Braunschweig: Vieweg 1979
10. Rand, R. H.: Computer algebra in applied mathematics: An introduction to MACSYMA. Boston, London, Melbourne: Pitman 1984

Received June 14, 1985

Prof. Dr. techn. U. Gamer
Technische Universität Wien
Institut für Mechanik
Karlsplatz 13
A-1040 Wien
Austria

Prof. Dr.-Ing. F. G. Kollmann
Technische Hochschule Darmstadt
Fachgebiet Maschinenelemente und Getriebe
Magdalenenstr. 8—10
D-6100 Darmstadt
Federal Republic of Germany